A Spectroscopic and Thermodynamic Study of Porphyrin/DNA Supramolecular Assemblies

Robert F. Pasternack,* Jonas I. Goldsmith,* Szilvia Szép,* and Esther J. Gibbs#
*Department of Chemistry, Swarthmore College, Swarthmore, Pennsylvania 19081 and #Department of Chemistry, Goucher College, Towson, Maryland 21204 USA

ABSTRACT Assemblies of *trans*-bis(*N*-methylpyridinium-4-yl)diphenylporphine ions on the surface of calf thymus DNA have been studied using several spectroscopic techniques: absorbance, circular dichroism, and resonance light scattering. The aggregation equilibrium can be treated as a two-state system—monomer and assembly—each bound to the nucleic acid template. The aggregate absorption spectrum in the Soret region is resolved into two bands of Lorentzian line shape, while the DNA-bound monomer spectrum in this region is composed of two Gaussian bands. The Beer-Lambert law is obeyed by both porphyrin forms. The assembly is also characterized by an extremely large, bisignate induced circular dichroism (CD) profile and by enhanced resonance light scattering (RLS). Both the CD and RLS intensities depend linearly on aggregate concentration. The RLS result is consistent with a model for the aggregates as being either of a characteristic size or of a fixed distribution of sizes, independent of total porphyrin concentration or ionic strength. Above threshold values of concentration and ionic strength, the mass action expression for the equilibrium has a particularly simple form: $K' = \mathrm{cac}^{-1}$; where cac is defined as the "critical assembly concentration." The dependence of the cac upon temperature and ionic strength (NaCl) has been investigated at a fixed DNA concentration. The value of the cac scales as the inverse square of the sodium chloride concentration and, from temperature dependence studies, the aggregation process is shown to be exothermic.

INTRODUCTION

Organized chromophore assemblies are a focus for current research in areas as diverse as light harvesting (Stewart and Fox, 1996), molecular electronics (Borovkov et al., 1996; Lindsey, 1991), nonlinear optics (Bjornholm et al., 1992), and chemotherapeutics (Biolo et al., 1994). Many of these investigations employ porphyrins and the closely related phthalocyanines; these intensely colored substances, and especially the porphyrins, are relatively easy to synthesize and "tune" through judicious selection of peripheral substituents and inserted metals (Pasternack and Gibbs, 1996). A number of the reported assemblies have involved covalent links among the chromophore units, their formation often involving difficult and elegant syntheses (Harriman and Sauvage, 1996). In others, advantage is taken of weak interactions to promote self-forming organized arrays (Pasternack et al., 1991; Gibbs et al., 1988; Marzilli et al., 1992). Our studies have emphasized the latter approach; the assemblies we are investigating form as a consequence of van der Waals forces, hydrogen bonding, hydrophobic interactions, and electrostatic effects. An advantage offered by such non-covalently driven assembly formation is that the aggregation process can be turned "on" or "off" through changes in solution conditions, thereby permitting investigations not only of spectral and luminescence properties of the arrays, but the thermodynamics and kinetics of their formation as well.

We use nucleic acid and polypeptide scaffolds to bind and organize porphyrins into extended arrays, and have studied the resultant species via absorption spectroscopy, circular dichroism (CD), and resonance light scattering (RLS) (Pasternack et al., 1990, 1991, 1993, 1996; Gibbs et al., 1988; Pasternack and Gibbs, 1993; Bustamante et al., 1994; Pasternack and Collings, 1995). Once a concentration and ionic strength are reached that are adequate to initiate the aggregation process, *trans*-bis(*N*-methylpyridinium-4-yl)diphenylporphine (t-H_2P_{agg}, Fig. 1), and its copper(II) derivative relocate from their intercalated and/or groove-bound positions to form an extended organized array on the biopolymeric backbone (Pasternack et al., 1991; Gibbs et al., 1988). Similar reaction patterns (i.e., monomers→organized assembly) have been observed for several porphyrin derivatives with single-stranded DNAs (Pasternack et al., 1990), RNAs (Pasternack et al., 1996), and polypeptides (Pasternack et al., 1991; Pasternack and Gibbs, 1993; Pancoska et al., 1990; Borissevitch et al., 1997). Other conditions remaining constant, the assemblies on polynucleotides form most readily in the order poly(rA) > poly(dA) > poly(dG-dC)$_2$ > calf thymus DNA > poly(dA-dT)$_2$. Both porphyrins, t-H_2P_{agg} and t-CuP_{agg}, can also aggregate in the absence of a polynucleotide or polypeptide backbone (Gibbs et al., 1988; Mallamace et al., 1996a, b). However, the information needed to form organized, chiral assemblies (as detected through the remarkably large CD signals observed for these species) is provided by the polymer; the polymeric scaffolds serve as "templates" for the organization process.

Received for publication 11 April 1997 and in final form 13 May 1998.
Address reprint requests to Dr. Robert F. Pasternack, Department of Chemistry, Swarthmore College, 500 College Avenue, Swarthmore, PA 19081. Tel.: 610-328-8559; Fax: 610-328-7355; E-mail: rpaster1@swarthmore.edu.

0006-3495/98/08/1024/08 $2.00

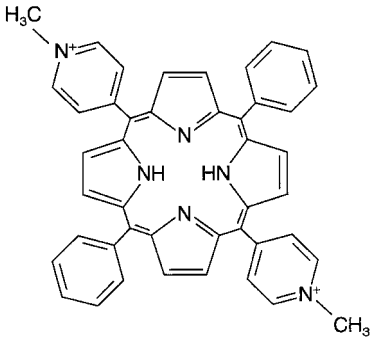

FIGURE 1 Structure of *trans*-bis(*N*-methylpyridinium-4-yl)diphenylporphine (t-H_2P_{agg}).

In the present work we examine the spectral characteristics of one such organized porphyrin assembly in greater detail than has been previously possible. The introduction of RLS as a standard spectroscopic method contributes to this fuller treatment. The outcome of these studies permits a consideration of the thermodynamics of the assembly process, including the form of the mass action expression.

MATERIALS AND METHODS

The porphyrin used for this study, t-H_2P_{agg} (Fig. 1), was obtained as the chloride salt from MidCentury Chemical (Posen, IL). Stock solutions, prepared from the solid in Millipore purified water, were stored in the dark. Porphyrin concentrations were determined in 1 mM phosphate buffer, pH~7, using a value for the molar absorptivity of $\epsilon = 2.40 \times 10^5\ M^{-1}\ cm^{-1}$ at the Soret maximum near 419 nm (Sari et al., 1990). Calf thymus DNA, obtained from Pharmacia Biotech (Piscataway, NJ) was purified using a standard method previously described (Pasternack et al., 1983). Concentrations, expressed in moles of basepairs per liter, were obtained using $\epsilon = 1.32 \times 10^4\ M^{-1}\ cm^{-1}$ at the DNA maximum, near 258 nm (Pachter et al., 1982). The integrity of the double helix was monitored via CD (Ivanov et al., 1973), with the expected $\Delta\epsilon \sim \pm 7\text{–}8\ M^{-1}\ cm^{-1}$ at the UV extrema.

Solutions were prepared by using a protocol in which the porphyrin was added to DNA in 1 mM phosphate buffer, pH~7; NaCl was always added last. We have shown previously that reproducible results are obtained when the porphyrin, in its monomeric form, is permitted to interact with the nucleic acid (Pasternack et al., 1991). The assembly process, initiated by the addition of electrolyte, is accomplished after the initial porphyrin/nucleic acid complex has formed.

Absorbance measurements were conducted on a JASCO V550 spectrophotometer using Fisher methacrylate cuvettes whenever possible. Porphyrin staining of the cuvette surface is less severe for methacrylate than when quartz cuvettes are used. The latter cuvettes, therefore, were reserved for experiments conducted in the UV region and for circular dichroism experiments performed on an Aviv 62DS Spectrometer. RLS measurements were conducted on a SPEX Fluorolog Spectrofluorimeter as previously described (Pasternack et al., 1993; Pasternack and Collings, 1995), using a "Synchronous Scan" mode. The emission and excitation monochromators were preset to identical wavelengths to determine the RLS spectrum. The RLS experimental spectra were corrected for absorption to obtain the "pure" scattering component. Two methods of correction were used. In the first, a standard approach generally used for dealing with primary and secondary shielding in fluorescence measurements was attempted except, in the present RLS case, the wavelength was the same for both corrections (Holland et al., 1977). Alternatively, a technique was developed to obtain the correction factor using a mixture of components, allowing the decoupling of the scattering signal from absorbance. We used samples of nonabsorbing polystyrene spheres of constant and readily determined scattering to which was added a known concentration of a dichromate solution. From the remeasured scattering and the absorbance of the dichromate solution, the correction factor as a function of absorbance could be computed. The form of the correction factor is given as $f(A) = 10^{-\mathbf{l}^* A}$, where $\mathbf{l}$ is an "effective" path length (which must be determined independently for each fluorimeter) and A is the absorbance. The details of this approach will be published separately.

Absorbance spectra of porphyrins bound to DNA were resolved into their component peaks using the *Peakfit* routine supplied by SPSS, Inc. (Chicago, IL). The monomer spectrum in the Soret region (from 350 nm to 500 nm) could be fit with two peaks of Gaussian line shape; a prominent one at 422 nm (G1) and a broad, less well-defined peak of considerably lower intensity, at 396 nm. When salt is added to the medium to promote porphyrin assembly, the Soret envelope becomes more complicated but could be fit consistently with four bands, two of Gaussian line shape corresponding in position and breadth to the two bands described above for the monomer and two additional bands of Lorentzian shape. One of these bands is prominent and centered at 449 nm (L1) while the other, at 367 nm, is quite broad and of lower intensity (Fig. 2). Attempts at fitting the spectra with bands exclusively of Gaussian line shape failed. The complete conversion of the monomer to aggregate requires a salt concentration that is sufficiently high that porphyrin/DNA binding would be weakened to a point at which much of the porphyrin is free in solution. Therefore, the molar absorptivities of aggregate/DNA peaks had to be determined indirectly (vide infra). The point to be emphasized here is that conditions for the experiments described below have been chosen so that, within experimental error, all the porphyrin remains associated with the DNA, whether acting as individual monomeric units or as part of an aggregate.

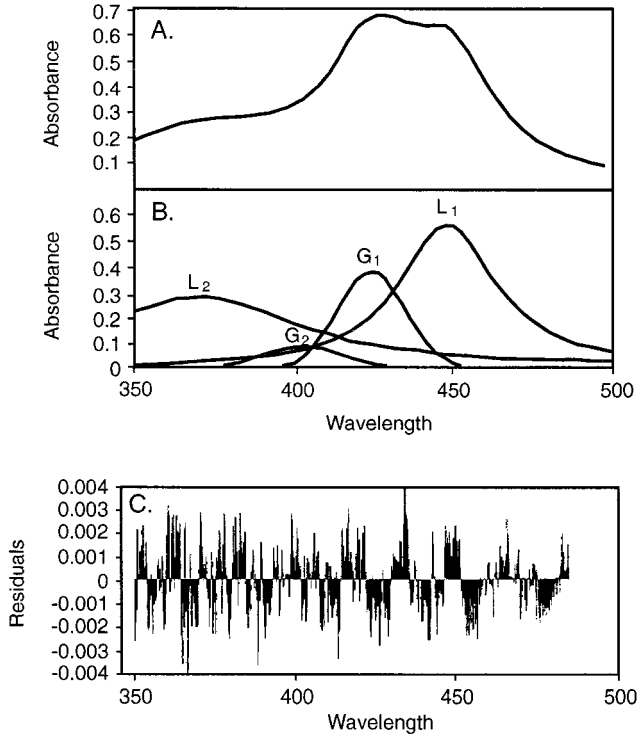

FIGURE 2 Absorption spectrum in the Soret region of a porphyrin/DNA solution containing both monomer and aggregate. (*A*) Experimental and theoretical spectra obtained with the spectral features shown in (*B*). The labeling of the peaks corresponds to the description in Materials and Methods. The residuals are shown in (*C*). These residuals are sufficiently small that the two spectra of (*A*) appear to coincide.

RESULTS

Absorption spectroscopy

Shown in Fig. 3 is the overlay of spectra of porphyrin/DNA solutions varying in NaCl concentration from 2 mM to 0.20 M. The porphyrin concentration is 5.5 μM, [DNA] = 40 μM, all in 1 mM phosphate buffer, 25°. Data used for this and subsequent analyses were restricted to conditions at which the porphyrin remains totally bound to the DNA (vide infra). As the salt concentration is raised from 2 mM to 0.20 M, the peak near 425 nm decreases in intensity while the one at 450 nm increases. An isosbestic point is obtained at 438 nm, suggesting a two-state model (monomer · DNA and aggregate · DNA) may be adequate for data analysis. From the monomer · DNA spectrum obtained at low salt concentration, the molar absorptivity for the *primary Gaussian peak* (G1, see Materials and Methods) was determined as $\epsilon_M = 1.17(\pm 0.02) \times 10^5\ M^{-1}\ cm^{-1}$ at 422 nm.

A conservation equation for porphyrin can be written for the putative two-state model as

$$C_o = [\text{Monomer} \cdot \text{DNA}] + [\text{Aggregate} \cdot \text{DNA}] \quad (1)$$

where C_o is total concentration of porphyrin and [Aggregate · DNA] is concentration of porphyrin arranged in aggregates, expressed as moles of porphyrin units/L. Then, for 1-cm cuvettes, if the Beer-Lambert law applies to the aggregate,

$$A_{G1} = \epsilon_M C_o - (\epsilon_M/\epsilon_{Agg})(A_{L1}) \quad (2)$$

where ϵ_{Agg} is the molar absorptivity of the primary Lorentzian band for the aggregated porphyrin at 449 nm. A_{G1} and A_{L1} are the intensities of the primary Gaussian (at 422 nm) and Lorentzian (at 449 nm) bands, respectively, obtained from the *Peakfit* routine. The plot of A_{G1} vs. A_{L1} proves to be linear (Fig. 3), confirming the applicability of the Beer-Lambert law for the aggregate peak at 449 nm, and providing a value of $\epsilon_{Agg} = 8.6(\pm 0.3) \times 10^4\ M^{-1}\ cm^{-1}$ for this spectral feature.

Resonance light scattering

The resonance light scattering (RLS) spectrum was obtained for each of the above samples. Fig. 4 provides an overlay of the *corrected* spectra (see Materials and Methods). The

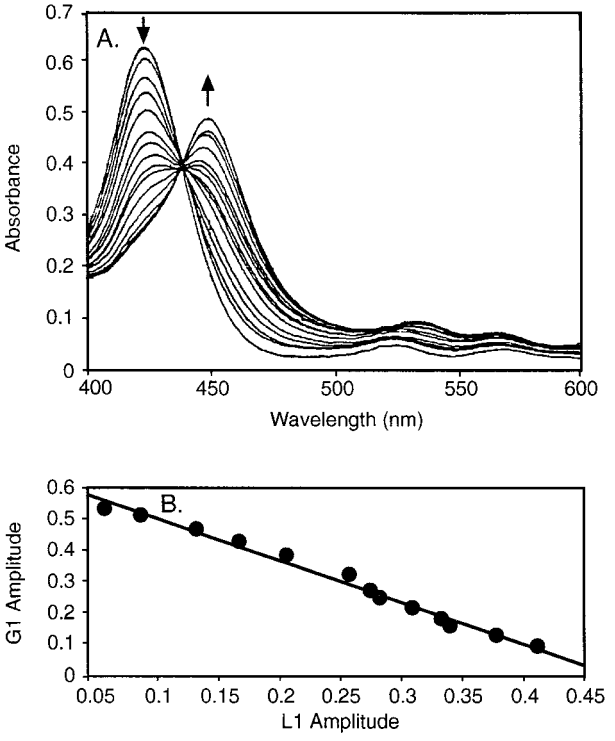

FIGURE 3 (*A*) Absorbance spectra of solutions containing 5.5 μM t-H_2P_{agg}, 40 μM DNA in 1 mM phosphate buffer at 25°. The NaCl concentration varies from 2.1 mM to 0.20 M. The band near 425 nm decreases while the one at 450 nm increases in intensity with increasing [NaCl]. (*B*) Plot of the amplitude of the 422 nm band (G1) versus that of the 449 nm band (L1) for the solutions shown in the upper portion of the figure. The slope of the line leads to a determination of $\epsilon_{Agg} = 8.6 \times 10^4\ M^{-1}\ cm^{-1}$.

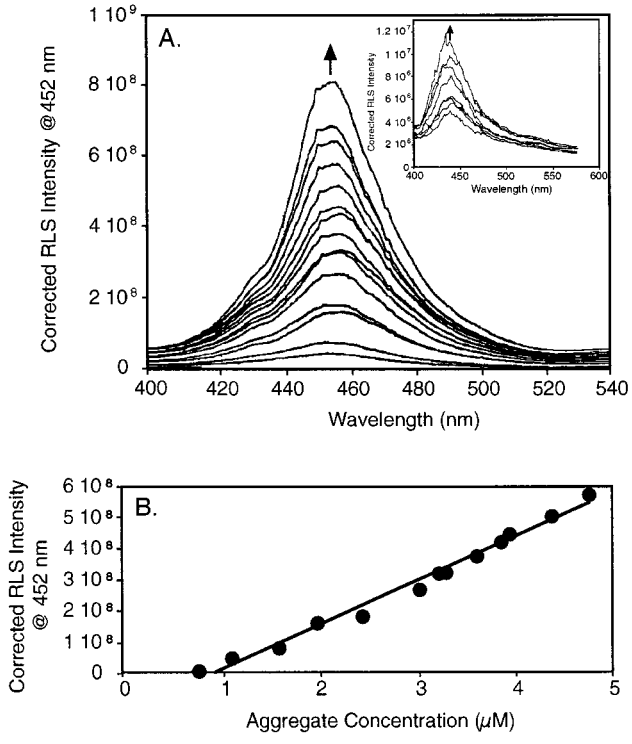

FIGURE 4 (*A*) Overlay of the RLS spectra for the solutions of Fig. 3 containing 5.5 μM t-H_2P_{agg}, 40 μM DNA in 1 mM phosphate buffer at 25°. The NaCl concentration varies from 2.1 mM to 0.20 M. These spectra have been corrected for absorbance as described in the text. *Inset:* Low ionic strength RLS spectra of solutions ranging in porphyrin concentration from 3.3 μM to 11 μM, [DNA] = 40 μM in 1 mM phosphate buffer. For these experiments, [NaCl] = 2.1 mM. The intensity of scattering is about two orders of magnitude smaller than that obtained at higher ionic strengths. For the solution containing 5.5 μM porphyrin, the intensity of scattering at low ionic strength is $\sim 5 \times 10^6$, and appears as near-zero on the lower plot. (*B*) Plot of corrected RLS intensity versus aggregate concentration for solutions in Fig. 3 ranging in [NaCl] from 2.1 mM to 0.10 M. The value of the slope of the line is 1.42×10^8 cps/μM.

signal, whose intensity increases with increasing [NaCl], is centered at 452 nm, near the λ_{max} associated with the aggregate. Using a combination of RLS and absorbance data, a plot was constructed for the corrected RLS intensity at the maximum versus aggregate concentration. As shown in Fig. 4, above a threshold value of $\sim 8 \times 10^{-7}$ M, the dependence appears linear, although the data are somewhat scattered. When the RLS spectra are obtained for porphyrin/DNA solutions under low ionic strength conditions, the signals are very small (although clearly above the background signal; see Fig. 4, *inset*) and centered at 435 nm. These results indicate that under low salt conditions, an aggregate is present having spectral features different from the major species produced at higher salt levels. For convenience, we refer to the major species as a type I assembly, while the low ionic strength form will be referred to as type II. That the absorbance spectra could be fit satisfactorily at low ionic strength without consideration of an aggregate form suggests that, consistent with the presence of an isosbestic point and the very small RLS and CD (vide infra) signals, type II aggregate concentrations are very low under the experimental conditions considered here. The type II aggregate can be detected because of the sensitivity of the latter two methods, compared to UV/vis absorption spectroscopy, in the presence of an extended electronically coupled aggregate.

Circular dichroism spectroscopy

Circular dichroism spectra were obtained from 350 nm to 550 nm for each sample, as shown in Fig. 5. The magnitude of both the positive and negative features for the bisignate signal increases with increasing salt concentration up to $\sim$0.15 M. Beyond that NaCl concentration, there is a *slight decrease* in the signal intensity, suggesting some dissociation of the porphyrin from the DNA template. Therefore, only solutions having [NaCl] below 0.15 M were used in this and the previously described analyses. Similar to the RLS results, above an aggregate concentration of 8×10^{-7} M, a linear dependence of the CD signal on aggregate concentration at both 432 nm (positive signal) and 455 nm (negative signal) is observed, having slopes of $\Delta\epsilon = +3200$ M^{-1} cm^{-1} and -4700 M^{-1} cm^{-1}, respectively.

The CD properties of the type II aggregate at low salt conditions were explored in some detail. Spectra were obtained at [NaCl] = 2.1 mM for solutions containing 40 μM DNA and varying porphyrin concentration from 3.3 to 11 μM. A bisignate CD profile, suggestive of an aggregate, could be detected especially toward the upper end of the range (see Fig. 5, *inset*). This CD profile is nearly conservative and of *opposite phasing* to that obtained at higher salt concentrations. We conclude that under these low salt conditions, the formed aggregate has a different orientation with respect to the DNA template from the type I assembly formed at higher [NaCl].

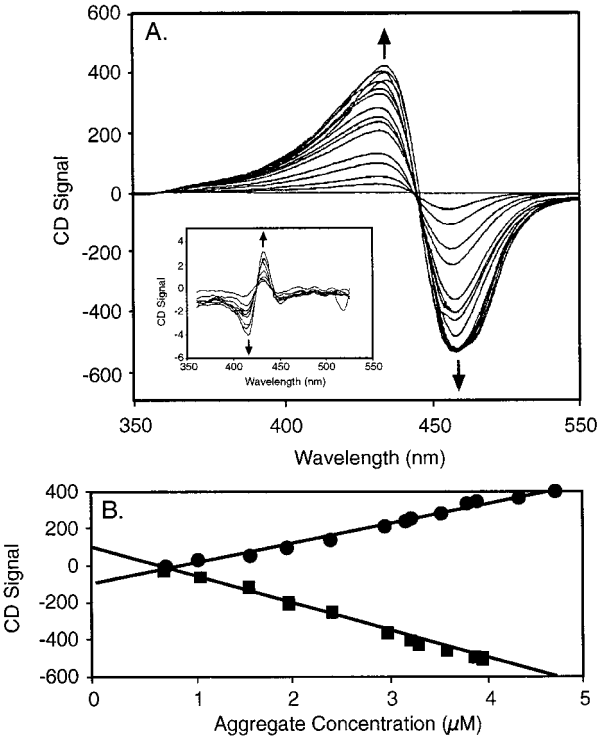

FIGURE 5 (*A*) Circular dichroism spectra overlay for samples of Fig. 3 containing 5.5 μM t-H_2P_{agg}, 40 μM DNA in 1 mM phosphate buffer at 25°. The NaCl concentration varies from 2.1 mM to 0.20 M. *Inset:* CD spectra of aggregates formed under low ionic strength conditions. These solutions range in porphyrin concentration from 3.3 μM to 11 μM, [DNA] = 40 μM in 1 mM phosphate buffer. The NaCl concentration is 2.1 mM. (*B*) Plot of the circular dichroism signals (in millidegrees) at 432 nm (positive signal) and 455 nm (negative signal) versus aggregate concentration. The slopes (in terms of $\Delta\epsilon$) are $+3200$ M^{-1} cm^{-1} and -4700 M^{-1} cm^{-1}, respectively.

Concentration dependencies

The effect of porphyrin concentration on the monomer/aggregate equilibrium was studied at several NaCl concentrations for the type I assembly. At each ionic strength, some eight to ten solutions varying in porphyrin concentration from 3.3 to 11 μM were considered; the DNA concentration was kept constant at 40 μM and the phosphate buffer at 1 mM, all at 25°. For each solution, the concentration of monomer and aggregate was determined as earlier, using the *Peakfit* routine. Results for representative NaCl concentrations are shown in Figs. 6 and 7 for the aggregate and monomer concentrations, respectively. The patterns observed in these figures are consistent with the assembly model proposed for this system. As the ionic strength increases for any given total porphyrin concentration, the aggregate concentration increases. Furthermore, as expected, the aggregate concentration at a given ionic strength increases with increasing total porphyrin concentration; gradually at low ionic strengths and more rapidly at higher values. In fact, as shown in Fig. 6, the slopes of the lines at ionic strengths of 0.087 and 0.10 are both unity (1.00 and 1.02), within experimental error. At these salt concentra-

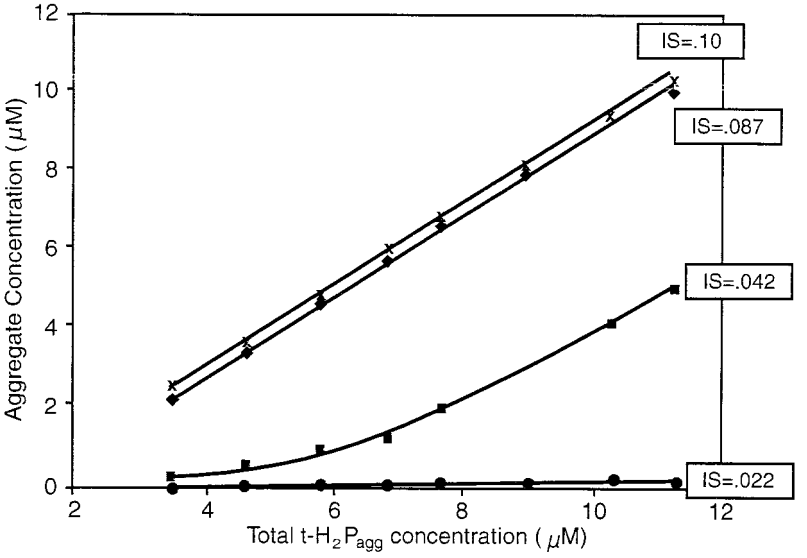

FIGURE 6 Plots of aggregate concentration versus total porphyrin concentration at representative ionic strengths (IS).

tions all added porphyrin contributes to the aggregate; the monomer concentration remains constant!

An examination of Fig. 7 confirms this conclusion. Whereas the monomer concentration increases markedly at low ionic strengths (the slope of the ionic strength = 0.0022 line is 0.96), at the highest ionic strengths studied, the monomer concentration remains unchanged as porphyrin is added. We refer to this fixed, limiting concentration as the "critical assembly concentration" (cac), the value of which depends on the sodium chloride concentration. At an intermediate ionic strength such as 0.042, the monomer concentration is seen to increase at first (see *inset*) but then level off to a value estimated as 6.6 μM for the cac.

Temperature dependence

A study of the influence of temperature on the monomer/aggregate equilibrium was conducted at an ionic strength of 0.082. Fig. 8 shows this influence qualitatively; as the temperature increases, the short wavelength band (due to monomer) increases at the expense of the long wavelength band (due to aggregate). The aggregation process is therefore revealed to be exothermic.

DISCUSSION

The accumulated spectroscopic evidence for the t-H_2P_{agg}/DNA system is consistent with a model in which—under appropriate conditions of ionic strength, concentration and temperature—extended porphyrin aggregates having long-range order are bound to the nucleic acid (Pasternack et al., 1991, 1993). The interactions with the biopolymer backbone are primarily electrostatic in nature; under conditions at which the porphyrin is extensively aggregated, *the nucleic acid CD spectrum* in the ultraviolet region resembles that of the native state. Furthermore, porphyrin assemblies

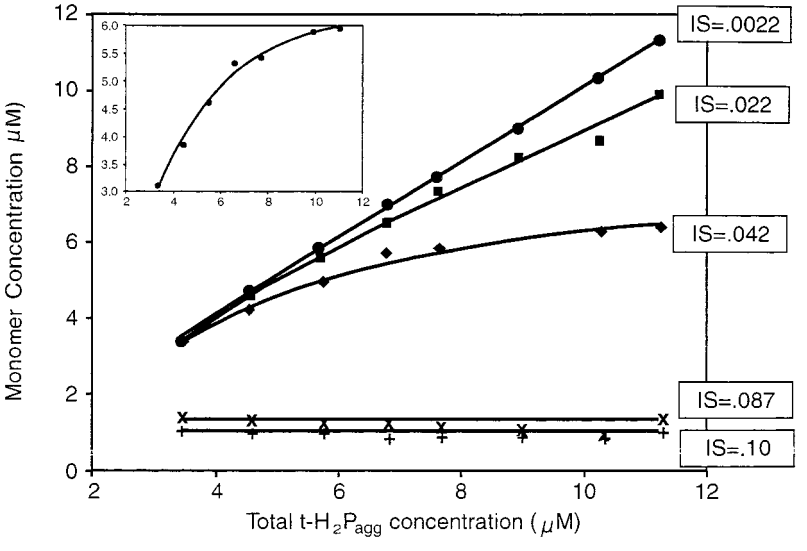

FIGURE 7 Plots of monomer concentration versus total porphyrin concentration at representative ionic strengths (IS). *Inset:* Determination of the cac at an ionic strength of 0.042 M.

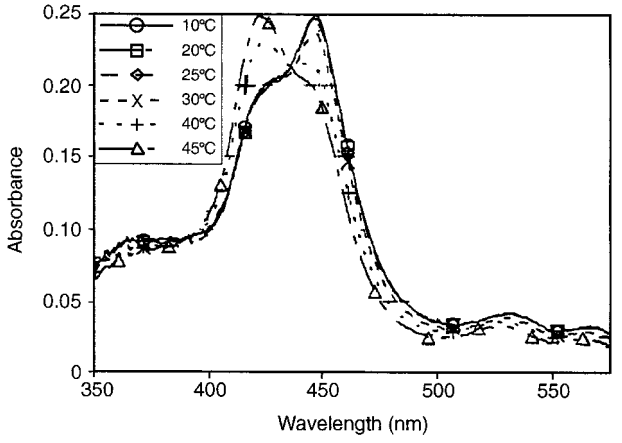

FIGURE 8 Absorbance spectra at several temperatures of a solution containing 2.9 μM porphyrin, 40 μM DNA, 1 mM phosphate buffer, and [NaCl] = 0.082 M. Increasing temperature promotes the bands associated with the monomer at the expense of the aggregate bands.

having similar absorbance, CD and RLS features can be formed on polypeptides as well as on polynucleotides (Pasternack et al., 1991; Pasternack and Gibbs, 1993) implying that the DNA bases are not playing a major role in the aggregation process. The dependence of the aggregation tendency on basepair composition described in the Introduction quite likely reflects the impact of the bases on the charge distribution, stability, and rigidity of the nucleic acid template. The magnitude of the CD and RLS signals in the Soret region indicate that the assembly can be considered as involving electronically coupled porphyrins behaving as a single unit; i.e., as an antenna. The results presented here describe the spectroscopic features of these arrays, and explore thermodynamic aspects of assembly formation.

The spectral bands due to the assembly do not conform to Gaussian profiles, similar to reports for other systems involving extended aggregate assemblies (Pasternack et al., 1972; Horng and Quitevis, 1993). Although referred to as absorption bands, the aggregate features described here are better thought of as "extinction bands" because they arise not only from absorption, but have a scattering contribution as well. The enormous enhancement in the *resonance* scattering spectrum is the consequence of a substantial increase in efficiency of scattering within the absorption envelope and, therefore, it is unwarranted to assume that only a negligible fraction of the photon flux is scattered in this range. As has been shown by others (Stanton et al., 1981), bands of Lorentzian (or the closely related Voigt) line shape are adequate (if only approximate, theoretically) when modeling such scattering components.

The intensity of the 449 nm Lorentzian feature (L1) is shown to depend linearly on the aggregate concentration, permitting the analyses of other spectral properties to be conducted as a function of *aggregate* concentration (in moles of monomer units/L contained in the extended assembly) rather than total porphyrin concentration. As shown in Figs. 4 and 5, a linear dependence of CD and RLS intensities on aggregate concentration is observed for this system. The simplicity of the dependence of the RLS intensity provides some insight into features of these assemblies. The excess resonance Rayleigh scattering intensity (I_x)—that is, the scattering beyond that provided by the medium—has been considered theoretically by Miller using macroscopic fluctuation theory (Miller, 1978). With this approach as a starting point, and noting that within the absorption envelope terms involving the imaginary part of the index of refraction (or polarizability) dominate, it can be shown that

$$I_X \sim \langle N \rangle \cdot \mathrm{Abs} \cdot \epsilon/\lambda_o^2 \qquad (3)$$

where $\langle N \rangle$ is the size of the aggregates expressed in monomer units. The linear dependence of the RLS intensity on [Aggregate]—which in turn, as seen in Fig. 4, is proportional to the absorbance—suggests that either the aggregates are of a single size or in some *fixed* distribution of sizes; in other words, $\langle N \rangle$ does not vary as a function of aggregate concentration. A similar conclusion, that the assemblies are of some characteristic size in solution under a variety of conditions, has been reached from studies involving both on- and off-resonance dynamic light scattering (Pasternack and Collings, 1995; Mallamace et al., 1996a, b).

An examination of CD and RLS spectral properties under conditions of low ionic strength demonstrates that an aggregate is present that differs in a number of respects from the one observed under more usual conditions. This low-salt aggregate (type II) has its absorption maximum at 435 nm (as indicated by the corrected RLS spectrum) and a CD profile of opposite phasing to that observed for the high-salt type I form. We propose that the low-salt aggregate involves a different orientation of the porphyrin with respect to the dyad axis of the polymer; and, since it is stable at low ionic strengths, possibly one that maximizes electrostatic interactions. The porphyrin may form a near "face-on" type complex in the type II aggregate with both of its $(+)N–CH_3$ groups in proximity to phosphates on the nucleic acid, while at higher ionic strengths the preferred orientation is likely to be "end-on." The modeling of a "face-on" type aggregate has been attempted (N. Gresh, personal communication) and it has been shown that such structures are possible, even for rigid DNA.

Returning to the type I porphyrin assembly formed under more typical salt conditions, analysis of the titration data in which either the NaCl concentration or porphyrin concentration is varied was carried out using a two-state model. Although most certainly an oversimplification, this approach proves successful, implying that the aggregates are sufficiently large that "end-effects" can be neglected; i.e., the main contributors to the spectral features are porphyrin monomers and *interior* porphyrin units in an extended aggregate. Application of Eq. 3 to this system confirms dynamic light scattering results that the porphyrin aggregates are very large, involving thousands of monomeric units. A critical assembly concentration can be defined for the type I aggregate, above which all added porphyrin becomes part

of the array. However, there is unequivocal evidence for the existence of porphyrin assemblies below the critical assembly concentration (cac), with added porphyrin distributing between monomer and aggregated forms (see Fig. 7, *inset*). The value of the cac depends on the salt concentration and temperature; plots of ln(cac) versus ln(ionic strength) and versus T^{-1} are both linear (Fig. 9) with slopes of -2.15 and -1070 Kelvin^{-1}, respectively.

In our studies of the kinetics of the assembly process (Pasternack et al., 1998), we find evidence for the formation of a critical nucleus that forms en route to the final assembly product. The existence of such a nucleus has an impact on both the thermodynamic and kinetic features of the aggregation process, as described by Oosawa and Kasai (1962). We define the nucleus as consisting of **m** monomeric units [**m** proves to be from 2 to 8 for the present system, depending on reaction conditions (Pasternack et al., 1998)]. The assumption is made that a single equilibrium constant, K, can be used for the stepwise aggregation until an **m**-mer is reached. This **m**-mer then undergoes some structural, positional, or orientational conversion (this step proves to be rate-determining in the kinetic scheme) to form a new species, $\langle M_m \rangle$, which then serves as the nucleus for further polymer growth to form the type I assembly. The addition of monomer units to the aggregate formed after the conversion is characterized by another stepwise equilibrium constant, K'. When $K' \gg K$, a critical assembly concentration can be defined (Oosawa and Kasai, 1962) as

$$\text{cac} = 1/K'(1 - K/K')^2 \qquad (4)$$

This model leads to the prediction that at total concentrations above the cac, only the assembly concentration increases with added porphyrin, at a constant concentration of DNA; this is precisely the pattern observed for the present system (Figs. 6 and 7). Although this approach is only approximate, it reveals the relationship of the dependence of cac upon ionic strength and temperature to thermodynamic parameters for the polymerization process. Therefore, estimating cac$\sim 1/K'$, the reciprocal of the post-nucleus type I equilibrium constant, we obtain that K' scales as $\sim$[NaCl]^2 and that the polymerization process is exothermic with $\Delta H^o \sim -9$ kJ/mole for monomer-binding to the type I aggregate.

In summary, we conclude that

- Long-range organized assemblies of porphyrins form spontaneously on helical polymers such as DNA as templates. The t-H_2P_{agg}/DNA system can be characterized by a two-state model: monomer and aggregate. The monomer has its primary Soret band at 422 nm ($\epsilon = 1.17 \times 10^5$ M^{-1} cm^{-1}), and the aggregate at 449 nm ($\epsilon = 8.6 \times 10^4$ M^{-1} cm^{-1}).
- The aggregated porphyrins are electronically coupled, having structural periodic repeats responsible for the large induced circular dichroism signals produced. This "resonance effect" arises from the interaction occurring over long distances; signals of this magnitude cannot be accounted for in terms of nearest-neighbor or next-to-nearest neighbor effects alone. The assembly behaves in this respect as an antenna, which is also the basis for the enhanced RLS observed.
- The mass action expression for porphyrin assembly can be written under appropriate conditions in terms of the critical assembly concentration alone. The value of the cac varies inversely as the electrolyte (NaCl) concentration to approximately the second power. The value of cac increases with increasing temperature, consistent with the observation that assembly formation is exothermic; the aggregate is stabilized by lowering the temperature, making the critical drug load more readily accessed.

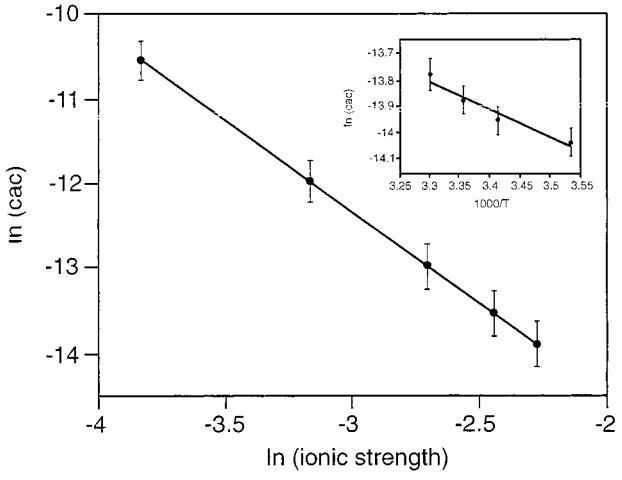

FIGURE 9 Plot of ln(cac) versus ln(ionic strength). The slope of the line is $-2.15(\pm.02)$ and the intercept is $-18.8(\pm.1)$. The error bars are obtained from the uncertainty in the cac at each ionic strength. *Inset:* Plot of ln(cac) versus T^{-1} giving a slope of $-1070(\pm 190)$ K^{-1}.

The authors thank Sean Ewen for confirming several of the spectral fits used in this analysis.

This work was supported by National Science Foundation Grant CHE-9510127 and the Howard Hughes Medical Institute.

REFERENCES

Biolo, R., G. Jori, M. Soncin, R. Pratesi, U. Vanni, B. Richter, M. E. Kenney, and M. A. Rodgers. 1994. Photodynamic therapy of B16 pigmented melanoma with liposome-delivered Si(IV)-naphthalocyanine. *Photochem. Photobiol.* 59:362–365.

Bjornholm, T., T. Geisler, J. Larsen, and M. Jorgensen. 1992. Nonlinear optical phenomena due to donor-acceptor interfaces created in Langmuir-Blodgett films. *J. Chem. Soc. Chem. Commun.* 815–817.

Borissevitch, I., Tominaga, T. T., Imasato, H., and Tabak, M. 1997. Resonance light scattering study of aggregation of two water soluble porphyrins due to their interaction with bovine serum albumin. *Anal. Chim. Acta*. 343:281–286.

Borovkov, V. V., M. Anikin, K. Wasa, and Y. Sakata. 1996. Structurally controlled porphyrin-aggregation process in phospholipid membranes. *Photochem. Photobiol.* 63:477–482.

Bustamante, C., S. Gurrieri, R. F. Pasternack, R. Purrello, and E. Rizzarelli. 1994. Interaction of water-soluble porphyrins with single- and double-stranded polyribonucleotides. *Biopolymers*. 34:1099–1104.

Gibbs, E. J., I. Tinoco, Jr., M. F. Maestre, P. A. Ellinas, and R. F. Pasternack. 1988. Self-assembly of porphyrins on nucleic acid templates. *Biochem. Biophys. Res. Commun.* 157:350–358.

Harriman, A., and J.-P. Sauvage. 1996. A strategy for constructing photosynthetic models: porphyrin-containing modules assembled around transition metals. *Chem. Soc. Rev.* 25:41–48.

Holland, J. F., R. E. Teets, P. M. Kelly, and A. Timmick. 1977. Correction of right-angle fluorescence measurements for the absorption of excitation radiation. *Anal. Chem.* 49:706–710.

Horng, M.-L., and E. L. Quitevis. 1993. Excited-state dynamics of polymer-bound J-aggregates. *J. Am. Chem. Soc.* 115:12408–12415.

Ivanov, V. I., L. E. Minchenkova, A. K. Schyolkina, and A. I. Poletayev. 1973. Different conformations of double-stranded nucleic acid in solution as revealed by circular dichroism. *Biopolymers*. 12:89–110.

Lindsey, J. S. 1991. Self-assembly in synthetic routes to molecular devices. Biological principles and chemical perspectives: a review. *New. J. Chem.* 15:153–180.

Mallamace, F., N. Micali, L. Monsu Scolaro, R. F. Pasternack, A. Romeo, A. Terracina, and S. Trusso. 1996b. Porphyrin aggregation in aqueous solutions: small angle and quasielastic light scattering. *J. Mol. Struct.* 383:255–260.

Mallamace, F., N. Micali, S. Trusso, L. Monsu Scolaro, A. Romeo, A. Terracina, and R. F. Pasternack. 1996a. Experimental evidence for self-similar structures in the aggregation of porphyrins in aqueous solutions. *Phys. Rev. Lett.* 76:4741–4744.

Marzilli, L. G., G. Petho, M. Lin, M. S. Kim, and D. W. Dixon. 1992. Tentacle porphyrins. DNA interactions. *J. Am. Chem. Soc.* 114: 7575–7577.

Miller, G. A. 1978. Fluctuation theory of the resonance enhancement of Rayleigh scattering in absorbing media. *J. Phys. Chem.* 82:616–618.

Oosawa, F., and M. Kasai. 1962. A theory of linear and helical aggregation of macromolecules. *J. Mol. Biol.* 4:10–21.

Pachter, J. A., C. H. Huang, V. H. Duvernay, A. W. Prestayko, and S. T. Crooke. 1982. Viscometric and fluorometric studies of deoxyribonucleic acid interactions of several new anthracyclines. *Biochemistry.* 21: 1541–1547.

Pancoska, P., M. Urbanova, L. Bednarova, K. Vacek, V. Z. Paschenko, S. Vasiliev, P. Malon, and M. Kral. 1990. Models of pigment-protein interactions in photosynthetic systems: tetraphenylporphine complexes with polycationic sequential polypeptides. Absorption, circular dichroism and fluorescence properties. *Chem. Phys.* 147:401–413.

Pasternack, R. F., R. A. Brigandi, M. J. Abrams, A. P. Williams, and E. J. Gibbs. 1990. Interactions of porphyrins and metalloporphyrins with single-stranded poly(dA). *Inorg. Chem.* 29:4483–4486.

Pasternack, R. F., C. Bustamante, P. J. Collings, A. Giannetto, and E. J. Gibbs. 1993. Porphyrin assemblies on DNA as studied by a resonance light-scattering technique. *J. Am. Chem. Soc.* 115:5393–5399.

Pasternack, R. F., and P. J. Collings. 1995. Resonance light scattering: a new technique for studying chromophore aggregation. *Science* 269: 935–939.

Pasternack, R. F., A. Giannetto, P. Pagano, and E. J. Gibbs. 1991. Self-assembly of porphyrins on nucleic acids and polypeptides. *J. Am. Chem. Soc.* 113:7799–7800.

Pasternack, R. F., and E. J. Gibbs. 1993. Porphyrin assembly formation on helical biopolymers. *J. Inorg. Organomet. Polymers*. 3:77–88.

Pasternack, R. F., and E. J. Gibbs. 1996. Porphyrin and metalloporphyrin interactions with nucleic acids. *In* Metal Ions in Biological Systems 33. Probing of Nucleic Acids by Metal Complexes of Small Molecules. A. Sigel and H. Sigel, editors. Marcel Dekker, Inc., New York. 367–397.

Pasternack, R. F., E. J. Gibbs, P. C. Collings, J. C. dePaula, L. C. Turzo, and A. Terracina. 1998. A non-conventional approach to supramolecular formation dynamics. The kinetics of assembly of DNA-bound porphyrins. *J. Am. Chem. Soc.* In press.

Pasternack, R. F., E. J. Gibbs, and J. J. Villafranca. 1983. Interactions of porphyrins with nucleic acids. *Biochemistry.* 22:2406–2414.

Pasternack, R. F., S. Gurrieri, R. Lauceri, and R. Purrello. 1996. Single-stranded nucleic acids as templates for porphyrin assembly formation. *Inorg. Chim. Acta*. 246:7–12.

Pasternack, R. F., P. R. Huber, P. Boyd, G. Engasser, L. Francesconi, E. Gibbs, P. Fasella, G. Cerio Venturo, and L. de C. Hinds. 1972. On the aggregation of meso-substituted water soluble porphyrins. *J. Am. Chem. Soc.* 94:4511–4517.

Sari, M. A., J. P. Battioni, D. Dupre, D. Mansuy, and J. B. Le Pecq. 1990. Interaction of cationic porphyrins with DNA. Importance of the number and position of the charges and minimum structural requirements for intercalation. *Biochemistry.* 29:4205–4215.

Stanton, S. G., R. Pecora, and B. S. Hudson. 1981. Resonance enhanced dynamic Rayleigh scattering. *J. Chem. Phys.* 75:5615–5626.

Stewart, G. M., and M. A. Fox. 1996. Chromophore-labeled dendrons on light harvesting antennae. *J. Am. Chem. Soc.* 118:4354–4360.